Encoding Circularity in Polydiketoenamine Thermoplastics via Oxy-Functionalization

Jeremy Demarteau[1], Alexander R. Epstein[2], Laura J. Reed,[1] Nicodemo R. Ciccia[3,4], John F. Hartwig[3,4], Kristin A. Persson[1,2], Brett A. Helms[1,5,6]*

[1]The Molecular Foundry, Lawrence Berkeley National Laboratory, Berkeley CA, 94720 USA.
[2]Department of Materials Sciences and Engineering, University of California, Berkeley CA, 94720 USA.
[3]Department of Chemistry, University of California, Berkeley; Berkeley, California 94720, United States.
[4]Division of Chemical Sciences, Lawrence Berkeley National Laboratory; Berkeley, California 94720, United States.
[5]Materials Sciences Division, Lawrence Berkeley National Laboratory, Berkeley CA, 94720 USA.
[6]Joint BioEnergy Institute, Emeryville, California 94608 USA.

*Correspondence: bahelms@lbl.gov

Abstract

Heteroatoms along polymer backbones permit selective controlled polymerization and depolymerization relevant to sustaining life, storing and retrieving information, as well as recycling and composting plastics. While structural biology has provided insight into how enzymes interact with heteroatoms in biopolymers to direct their transformations, there remains much to be learned from related investigations for synthetic polymers, where conformational space sampled by chains is expected to play a more prominent role in governing polymer reactivity in the absence of enzymes. Here, we show that oxy-functionalization at specific sites along polydiketoenamine (PDK) backbones affects depolymerization rates by over three orders of magnitude, due to differences in distortion energies associated with reactive chain conformations in transition states for acidolysis. Site-specific oxy-functionalization, resulting in the fastest rates of acidolysis, opens the door to deconstructing linear PDK chain topologies for the first time, broadening the scope of applications for PDK plastics in a circular manufacturing economy, including chemically recyclable adhesives for a diverse range of surfaces.

Main

Encoding circularity in polymers is important for enabling and perfecting the chemical recycling of plastic waste[1–4]. However, monomer-to-monomer circularity remains out of reach for the most widely used plastics, particularly polyethylene and polypropylene, due to their lack of readily

https://doi.org/10.26434/chemrxiv-2024-p5q4d **ORCID:** https://orcid.org/0000-0003-3925-4174 Content not peer-reviewed by ChemRxiv. **License:** CC BY-NC-ND 4.0

cleavable bonds[5]. Introducing heteroatoms as cleavage sites along polymer backbones has emerged as a versatile solution[6–8]—reminiscent of how circularity is achieved with biopolymers in living systems[9,10]. Yet, it remains unclear how the proximity of polar functionality near cleavage sites affects hydrolysis rates in aqueous media, where a diverse range of intermolecular interactions can alter reaction coordinates, conformations, and energy landscapes governing the rate-limiting step. If this were understood, it would be possible to deconstruct plastics to specific monomers or even oligomers at tunable fast rates.

Here, we show that oxy-functionalization of amine and triketone monomers at specific sites near acid-cleavable diketoenamine (DKE) bonds results in polydiketoenamine (PDK) deconstruction rates that are tunable over three orders of magnitude (**Fig. 1a**), enabling the creation of circular PDK thermoplastics and adhesives therefrom. To inform the basis by which oxy-functionalization might give rise to tunable deconstruction rates, we modeled the transition states for a series of oxy-functionalized DKE molecules and calculated the standard free energies of activation for hydrolysis, which differed by up to 20.6 kJ mol^{-1} due to structural changes between reactive conformations. To varying degrees by each DKE variant, an incoming water molecule could be guided to the iminium reaction center by hydrogen bonding, balancing energetic contributions for intermolecular interactions and intramolecular distortion, ultimately lowering free-energy barriers and increasing reaction rates. We synthesized the corresponding polymers and evaluated their deconstruction behaviors in strong aqueous acid. Most notably, while we verified the computational predictions, we found that the extent of depolymerization to triketone and amine monomers was complete only for specific designs, being informative for this emerging family of circular materials. We were also able to deconstruct PDK co-polymers at specific sites, exploiting differences in hydrolysis rates for each co-monomer. Encoding circularity in PDK through oxy-functionalization, optionally returning monomers or oligomers of defined length, is enabling in that chemical waste produced when recycling polymers is ultimately tied to the number of bonds breaking and reforming in the circular polymer lifecycle. We also find that oxy-functionalization improves the strength of PDK thermoplastics when they are used as hot-melt adhesives to a diverse range of substrates, particularly glass.

https://doi.org/10.26434/chemrxiv-2024-p5q4d **ORCID:** https://orcid.org/0000-0003-3925-4174 Content not peer-reviewed by ChemRxiv. **License:** CC BY-NC-ND 4.0

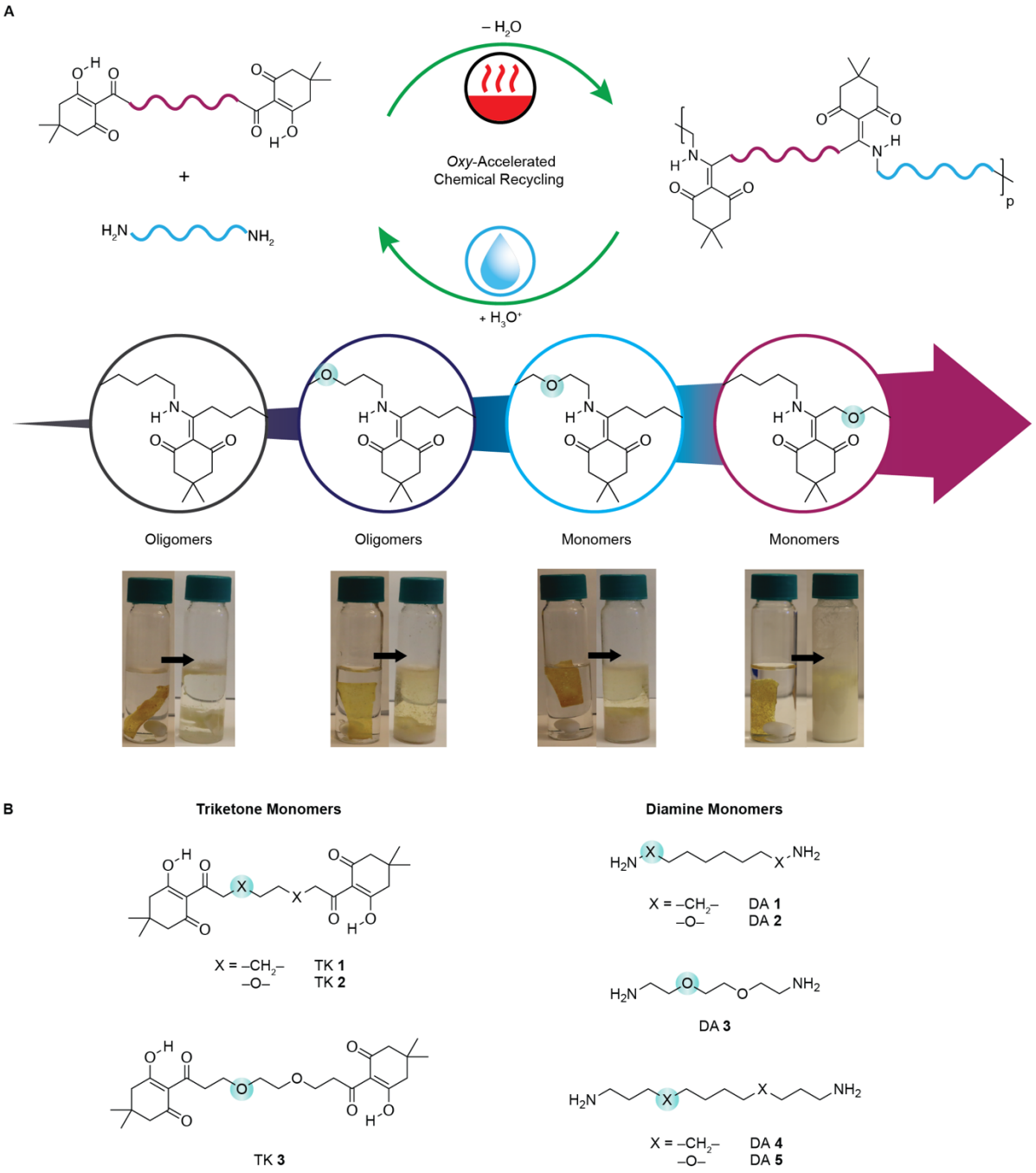

Fig. 1. Encoding circularity in polydiketoenamine thermoplastics. a, Oxy-functionalization of polydiketoenamines (PDK) enables closed-loop chemical recycling of thermoplastics at tunable fast rates via control over reactive polymer chain conformations in acidolytic media. **b**, Heteroatom-free and oxy-functionalized triketone and amine monomers used in the creation of circular PDK thermoplastics and adhesives.

https://doi.org/10.26434/chemrxiv-2024-p5q4d **ORCID:** https://orcid.org/0000-0003-3925-4174 Content not peer-reviewed by ChemRxiv. **License:** CC BY-NC-ND 4.0

This expanded family of circular PDK thermoplastics complements a growing number of chemically recyclable polymers that exploit heteroatoms to encode circularity, including polyesters[6,7,11–20], polythioesters[21–23], polycarbonates[24–27], polythiocarbonates[28], polyethers[8,29], polythioethers[30], polydisulfides[31–33] and polyamides[34–36]. In those studies, remarkable insights into monomer designs have made it possible to controllably polymerize and depolymerize plastics, many of which also exhibit useful properties[3,37]. Here, we go further by highlighting the profound importance of remote substituent effects on the lability of cleavable bonds in condensation polymers via control over reactive chain conformations, which has largely been underexplored. With this approach, we can achieve high rates, yields, and purities for the recovered monomers, while also uncovering the design rules for circularity with both molecular and macromolecular precision.

Results and discussion

Until now, circularity in PDK resins had been demonstrated for crosslinked thermosets, elastomers, and filled rubbers[38,43]. For those materials, chemical recycling to monomer was aided by a proximal tertiary amine in polytopic amine crosslinkers (e.g., *tris*(2-aminoethyl)amine, *tris*(3-aminopropyl)amine, etc.) used to create them[44]. Because tertiary amines are absent in most diamine monomers, it is necessary to recapitulate their function in lowering the standard free energy barriers to diketoenamine acidolysis. We hypothesized that a similar low barrier might be achieved through oxy-functionalization of the diamine; moreover, we also considered whether such similar effect might be gained by oxy-functionalized triketone monomers. The latter approach would be particularly attractive in that the diamine monomer would no longer require oxy-functionalization, since the oxy-group would be located on the triketone monomers. It would therefore become possible to use simpler diamines to formulate PDK thermoplastics with different properties without sacrificing circularity.

Yet, it was unclear how oxy-functionalization of amine or triketone monomers at specific sites might influence hydrolysis rates through pre-organization of the transition state. Previous insights had focused on a proximal amine, which in its ionized state served as a hydrogen-bond donor, leading water (as hydrogen-bond acceptor) to a reactive iminium intermediate along the reaction coordinate. Because oxy-functionalization installs a remote substituent that instead serves as hydrogen-bond acceptor, this inversion of the role of hydrogen bond donors and acceptors required

https://doi.org/10.26434/chemrxiv-2024-p5q4d **ORCID:** https://orcid.org/0000-0003-3925-4174 Content not peer-reviewed by ChemRxiv. **License:** CC BY-NC-ND 4.0

further investigation for understanding and controlling its influence on diketoenamine acidolysis rates. This motivated us to consider the implications of oxy-functionalization on the structure of the transition state during diketoenamine acidolysis.

To test these hypotheses, we determined the ensemble of lowest energy structures of ionized iminium intermediates and their subsequent transition states during acidolysis for small molecule diketoenamines, whose 1-hexylamine bonding partner featured either no oxy-functionalization (DKE **1**) or site-specific oxy-functionalization within 1, 2, 3, or 4 conjoining bonds of the nitrogen (DKE **2**–**5**, respectively). We generated these ensembles using the conformer–rotamer sampling tool (CREST)[45] and refined their free energies using hybrid density functional theory (DFT). We then calculated the hydrolysis reaction rate with multi-path transition state theory (MP-TST)[46,47], which we have found provides excellent agreement with experimental results for DKE hydrolysis by including statistics from higher-energy reactive pathways[44] (**Supplementary Fig. 1**). We then examined the relative rates of acidolysis ($k/k_{control}$) for oxy-functionalized diketoenamines **2**–**5**, using the rate for un-modified DKE **1** as the control ($k_{control}$) (**Fig. 2a**).

Through this analysis, we found that all oxy-functionalized derivatives delivered rate increases over the unmodified control, which were concurrent with stabilizing hydrogen bonds between the sites of oxy-functionalization and the attacking water molecule. Yet, these rate increases were not uniform. The behavior overall was non-monotonic, with DKE **3** and **4** delivering the highest rate increases by over three orders of magnitude. To understand this trend, we examined more closely the atomic configurations during the addition of water to the iminium (**Supplementary Fig. 2**).

The computations suggest that two competing factors contribute to the extent of stabilization: first, the distance (d) between the site of oxy-functionalization and the nearest hydrogen in the attacking water molecule, where stronger dispersion interactions led to a shorter stronger bond; and second, the torsion angle ϕ(C=C–C=N) of the iminium in its reactive conformation, where a larger torsion angle resulted in a larger energetic penalty to reach the lowest-energy transition state (**Supplementary Fig. 2**). We observed that when no methylene unit was present between the amine and the site of oxy-functionalization (DKE **2**), the interatomic distance between the site of oxy-functionalization and the closest hydrogen atom in water was too long in the transition state to establish a hydrogen bond. However, as the number of methylene spacers between the site of oxy-functionalization from the reaction center increased, d decreased and plateaued at a length characteristic of a hydrogen-bond, stabilizing the transition state. However, for DKE **4** and DKE

https://doi.org/10.26434/chemrxiv-2024-p5q4d **ORCID:** https://orcid.org/0000-0003-3925-4174 Content not peer-reviewed by ChemRxiv. **License:** CC BY-NC-ND 4.0

5, the torsion angle required to achieve a hydrogen-bonded reactive configuration substantially increased. Thus, the energetic stabilization from the hydrogen bond is partially cancelled by the strain energy to achieve a reactive conformation. Therefore, there are optimal sites for oxy-functionality in DKE molecules (i.e., DKE **4**) and likely motifs in polymers based on them that balance stabilization and strain.

To understand whether the placement of oxy-functionalization in the triketone might achieve a similar balance, we performed the same sequence of calculations on DKE **6**–**9**, where DKE **6** served as an unmodified control and DKE **7**–**9** featured oxy-functionalization at progressively longer spacing along the triketone (**Fig. 2b**). We found that the highest rates of acidolysis were predicted for DKE **8** and DKE **9**. The reactive conformations in their lowest-energy transition states for DKE **7**–**9** revealed a similar trend to that for DKE **2**–**5**: DKE **9** forms a hydrogen bond with the attacking water, increasing the acidolysis rate, whereas DKE **7** and DKE **8** have weaker dispersion interactions (**Supplementary Fig. 2**). The most significant difference from these trends was observed for DKE **7**, where the computed acidolysis rate is suppressed relative to the unmodified control. Here, oxy-functionalization directly affects the electronic structure at the reaction center.

https://doi.org/10.26434/chemrxiv-2024-p5q4d **ORCID:** https://orcid.org/0000-0003-3925-4174 Content not peer-reviewed by ChemRxiv. **License:** CC BY-NC-ND 4.0

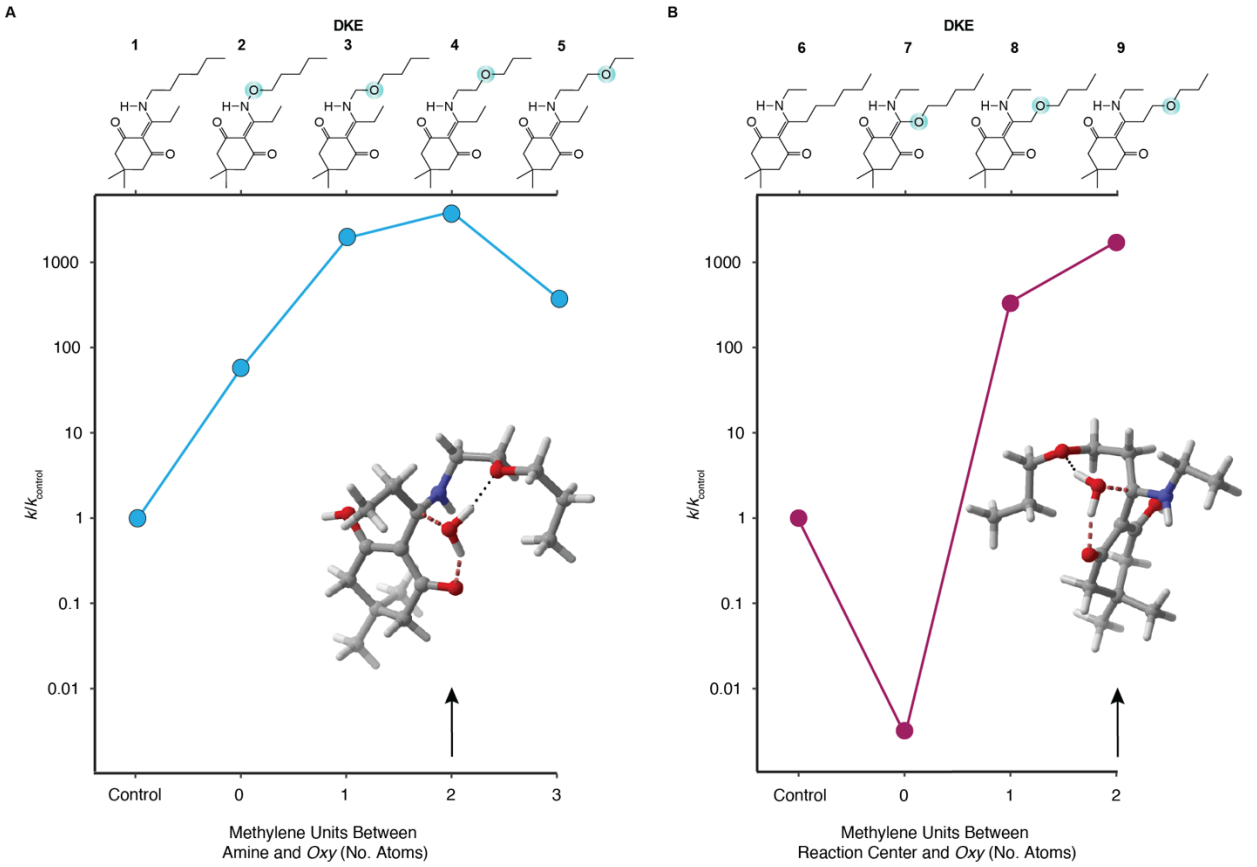

Fig. 2. **Relative rates of hydrolysis for oxy-functionalized diketoenamines. a**, Relative rates of hydrolysis for DKE **1–5**, which are differentiated on the manner and placement of oxy-functionality in the amine coupling partner. Relative rates are normalized to DKE **1** as the control. **b**, Relative rates of hydrolysis for DKE **6–9**, which are differentiated on the manner and placement of oxy-functionality in the triketone coupling partner. Relative rates are normalized to DKE **6** as the control.

To assess the validity of these theoretical predictions that oxy-functionalization of amine and triketone monomers accelerates DKE hydrolysis rates, we synthesized from a selection of three triketones and five diamines (**Fig. 1b**) a focused series of PDK resins **1**–**7** (**Fig. 3a**) via "click" polycondensation. This focus reflects a few key observations we made during our investigations. We noted thermal instability of PDK materials generated using alkoxymethanamines, having similar structural characteristics to DKE **3**; bonding motifs of that type were therefore not carried forward. Likewise, we did not further explore PDK designs based on bonding motifs similar to DKE **7**, since those materials are known to undergo amine exchange twice, liberating the alcohol[48–50]. This behavior does not permit retention of oxy-functionalization after polymerization; the

https://doi.org/10.26434/chemrxiv-2024-p5q4d **ORCID:** https://orcid.org/0000-0003-3925-4174 Content not peer-reviewed by ChemRxiv. **License:** CC BY-NC-ND 4.0

hypothetical PDK hydrolysis behavior is therefore untestable. With these considerations as a guide, we synthesized PDK **1**–**7** with molar masses (M_w) of 10–46 kg mol^{-1}. We also determined their glass transition temperatures (T_g) by differential scanning calorimetry: T_g values ranged from 16–63 °C (**Supplementary Table 1** & **Supplementary Figs. 4**–**6**). We could conduct the polymerization in solution or in polymer melts (**Supplementary Fig. 3**). However, we found that for PDK **2**, **6**, and **7**, addition of a solvent is beneficial, favoring higher degrees of polymerization (**Supplementary Table 2** and **Supplementary Fig. 7**).

We observed the deconstruction behaviors of PDK **1**–**7** in 5.0 M HCl at 20 °C for 96 h (**Fig. 3A**). With regard to changes in physical states of the polymers undergoing acidolysis and the accompanying monomers generated therefrom, there were strikingly different behaviors for the unmodified control compared to oxy-functionalized polymers. For PDK **1** and PDK **4**, which do not feature any oxy-functionalization in either amine or triketone monomers, we observed a transition from a solid densified polymer sample suspended in the reaction medium to a viscous liquid, suggesting possible ionization, but little or no hydrolysis, i.e., the ionized polyelectrolyte served primarily as a viscosity modifier to the reaction medium. On the other hand, for oxy-functionalized PDK **3** and PDK **5–7**, we observed that after ionization and solubilization of polymer chains, the liberated triketones became apparent as dispersed solids in the reaction medium, yet at different times for variants within the series. PDK **3** and PDK **6** stood out for their fast progression from dense solids to ionized and then soluble polymers undergoing hydrolysis; we observed dispersed triketone monomers after hydrolysis was complete.

In support of this interpretation of the visual progression, we confirmed by ^{1}H NMR the chemical identities of the dispersed solids after filtration and drying as the original triketone monomers (**Supplementary Figs. 8** & **9**). For quantitative analysis of PDK deconstruction behaviors, we calculated the percent conversion from recovered solids, taking account of the triketone-to-oligomer ratio from the accompanying ^{1}H NMR data (**Fig. 3b** & **Supplementary Figs. 10–16**); the chemical shift for hydrogen-bound O–H in the triketone monomer is at δ 17–19 ppm, while that for the hydrogen-bound N–H in oligomeric diketoenamines is at δ 12–16 ppm.

https://doi.org/10.26434/chemrxiv-2024-p5q4d **ORCID:** https://orcid.org/0000-0003-3925-4174 Content not peer-reviewed by ChemRxiv. **License:** CC BY-NC-ND 4.0

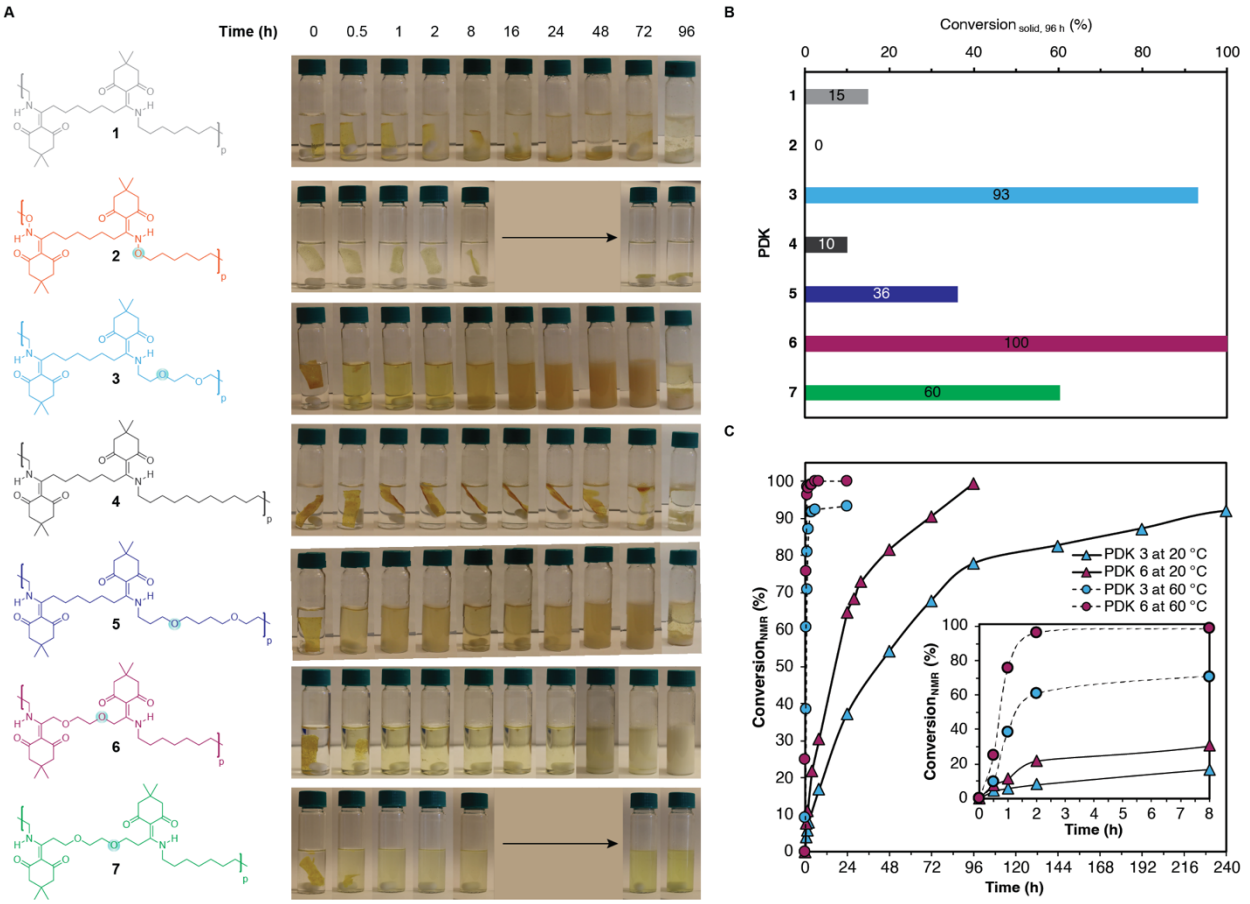

Fig. 3. Chemical recycling of PDK 1–7 thermoplastics in strong aqueous acid. a, Visual progression of the depolymerization trajectory over time. **b**, Conversion of PDK resins to monomer after 96 h in 5.0 M HCl at 20 °C. **c**, Divergent conversion rates of oxy-functionalized PDK **3** and **6** to monomer over time in 5.0 M HCl at either 20 °C or 60 °C, showcasing the benefits of implementing oxy-functionalized triketone monomers to facilitate PDK deconstruction at the fastest rates in the highest yields at the lowest temperature.

We found that conversions for PDK **1** and PDK **4** bearing no oxy-functionalization were less than 16% by ^{1}H NMR, consistent with our predictions that acidolysis rates would be slow. On the other hand, PDK **3** containing oxy-functionalized amine monomers achieved 93% conversion, consistent with the theoretical prediction of a markedly faster rate. Increasing the number of methylenes between the diketoenamine bond and the site of oxy-functionalization in the amine monomer led to a notable reduction in conversion as predicted, with PDK **5** achieving only 36% conversion after 96 h. However, no deconstruction of PDK **2** occurred under these reaction

https://doi.org/10.26434/chemrxiv-2024-p5q4d **ORCID:** https://orcid.org/0000-0003-3925-4174 Content not peer-reviewed by ChemRxiv. **License:** CC BY-NC-ND 4.0

conditions, deviating substantially with regard to theory. For PDK **6** and PDK **7** bearing oxy-functionality in the triketone monomer, we found conversions of 100% and 60%, respectively. While the structural integrity of recovered TK **2** monomer from PDK **6** was pristine after chemical recycling (**Supplementary Fig. 15**), TK **3** recovered from PDK **7** exhibited signs of chemical degradation due to retro-Michael reactions with the appearance of multiple peaks in the δ 17–19 ppm region (**Supplementary Fig. 16**).

Interestingly, even if deconstruction was relatively fast in the initial stages, depending on the site of oxy-functionalization within amine or triketone monomers, we recovered either exclusively the original triketone and amine monomers after acidolysis as desired, or monomers contaminated with oligomeric impurities (**Supplementary Figs. 10–14**). To understand the implications of these behaviors at different reaction temperatures, we quantified the isolated monomer yields and monomer:oligomer ratios for PDK **3,** prepared with the fastest-to-deconstruct oxy-functionalized diamine monomer DA **3,** and PDK **6,** prepared with the fastest-to-deconstruct oxy-functionalized ditopic triketone monomer TK **2**. When deconstructed at ambient temperature, PDK **3** returned solids with an overall conversion of 71%, yet a monomer-to-oligomer ratio of 93:7 (**Supplementary Fig. 12**). Increasing the temperature to 60 °C resulted in a 99:1 monomer-to-oligomer ratio. Acidolysis of PDK **6**, on the other hand, gave an 86% isolated yield of monomer with no oligomer impurities (**Supplementary Fig. 15**). This is further corroborated by monitoring and tracking conversion, monomer:oligomer ratios, and isolated triketone yields for PDK **3** and PDK **6** deconstruction at either 20 °C or 60 °C (**Fig. 3c**). At 20 °C, PDK **6** achieved 90% conversion of diketoenamine bonds to triketones within 72 h; PDK **3** required 10 days to reach the same conversion. At 60 °C, PDK **6** reached complete conversion in only 2 h; PDK **3** reached 93% conversion after 24 h.

In short, if the goal is to deconstruct PDK resins with linear topologies at the fastest possible rates with exclusive monomer recovery in high yield and high purity, we recommend that oxy-functionalization of amine monomers is preferred with only two methylenes separating the amine and ether functionalities. Ideally, however, we suggest oxy-functionalization of the triketone monomer with a single methylene spacer between the exocyclic ketone and ether functionalities. Acidolysis rates are substantially faster with PDK **6** (and likely variants thereof), monomers are recovered in the highest yield and purity, and, when practiced at scale, the shorter residence time in the reactor ultimately lowers the costs of chemical recycling[51,52].

https://doi.org/10.26434/chemrxiv-2024-p5q4d **ORCID:** https://orcid.org/0000-0003-3925-4174 Content not peer-reviewed by ChemRxiv. **License:** CC BY-NC-ND 4.0

We recognize that this recommendation will most likely appeal to those interested in recovering exclusively monomers when chemically recycling plastics. Nonetheless, this knowledgebase of polymer reactivity also suggests it should be possible to control which bonds in PDK chains hydrolyze, e.g., through copolymers where oxy-functionalization is introduced at intervals determined by monomer placement within the chain, on the basis of the more favorable energetics associated with the reactive conformation of the polymer in acid. This is underexplored in synthetic polymers, yet a natural consequence of requirements for transition-state pre-organization. In other words, oxy-functionalization encodes when and where the PDK chain is kinetically likely to cleave under experimentally accessible reactions conditions due to the effects of oxy-functionalization on the local chain conformation in acidolytic media, rather than the intrinsic lability of the cleavable bond in the absence of oxy-functionalization.

To demonstrate that PDK circularity is encodable via oxy-functionalization, we introduced oxy-functionalized TK **2** as a preferred cleavage site in otherwise slow-to-deconstruct PDK chains comprising TK **1** and DA **4** monomers (**Fig. 4a**): PDK **8**–**11** comprising 0.02, 0.07, 0.24 and 0.37 equivalents of TK **2**, respectively, exhibited molar masses ranging from 85–158 kg mol^{-1} (**Supplementary Fig. 17** and **Supplementary Table 3**). After deconstruction at 20 °C in 5.0 M HCl (**Fig. 4b**), heteroatom-free PDK **8** exhibited minimal physical changes as expected, while PDK **11** with 37% oxy-functionalization in the triketone monomer feed lost its original shape and exhibited features reminiscent of a soft hydrogel. This is consistent with the expectation that deconstruction at the preferred sites produces oligomers of defined length, depending on extent of oxy-functionalization. To support this interpretation, we assessed the molar masses of the deconstructed PDK **8**–**11** after deconstruction by size-exclusion chromatography (SEC) (**Supplementary Fig. 18** and **Supplementary Table 3**). We found that the ratio of final to initial molar masses indeed scaled with the extent of oxy-functionalized TK **2** monomer in the feed ratio (**Fig. 4c**).

https://doi.org/10.26434/chemrxiv-2024-p5q4d **ORCID:** https://orcid.org/0000-0003-3925-4174 Content not peer-reviewed by ChemRxiv. **License:** CC BY-NC-ND 4.0

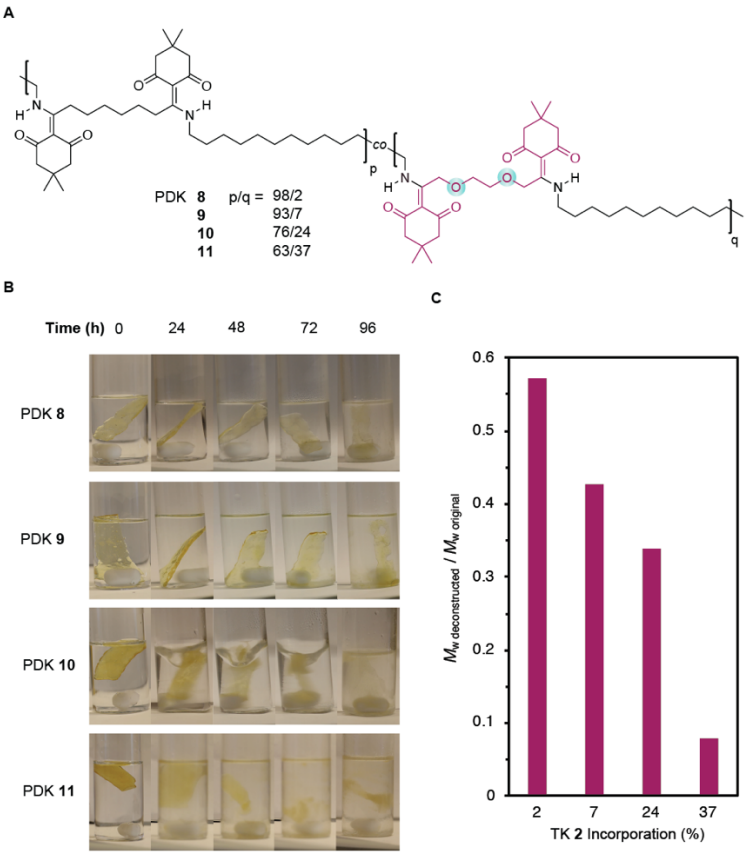

Fig. 4. Depolymerization of oxy-functionalized co-polymers PDK 8–11 thermoplastics in strong aqueous acid. a, The extent of oxy-functionalization was encoded by the relative amount of TK **1** and **2** in the monomer feed alongside DA **4**. **b**, Visual trajectory of the chemical depolymerization of PDK **8**–**11** over time in 5.0 M HCl at 20 °C. **c**, Ratio of deconstructed molar mass to the initial molar mass of PDK **8**–**11** as a function of TK **2** incorporation.

Considering the thermal properties of these PDK thermoplastics (T_g = 16–63 °C), their adhesive properties may be of interest. Hot melt adhesives typically comprise epoxies or polyurethanes, which struggle to close the loop in chemical recycling[53]. As such, most complicate recycling efforts for materials in bonded assemblies, including aluminum, polymers, glass, and stainless steel. We bonded pairs of substrates taken from aluminum, nylon 6,6, glass, or stainless steel. As test cases, we initially used either heteroatom-free PDK **1** or oxy-functionalized PDK **3** (**Fig. 5a** and **Supplementary Table 4**) as the hot melt adhesive. We identified glass substrates as having the best adhesive properties, with the lap shear strength averaging ~11.1 MPa for oxy-functionalized PDK **3**. Across all substrate types, oxy-functionalized PDK **3** consistently showed

https://doi.org/10.26434/chemrxiv-2024-p5q4d **ORCID:** https://orcid.org/0000-0003-3925-4174 Content not peer-reviewed by ChemRxiv. **License:** CC BY-NC-ND 4.0

higher values compared to heteroatom-free PDK **1**, suggesting a general positive influence of oxy-functionalization on enhancing adhesion strength compared to its exact heteroatom-free analogue.

To verify this hypothesis across the entire series, we performed tests for the lap shear strength for pairs of glass substrates bonded together by PDK adhesives. In standardized tests with adhesives configured with rectangular areas, lap shear tests of PDKs **3**–**6** consistently caused the bonded assemblies to fail due to excessive adhesive force (i.e., their lap shear strength was too high). We reduced the test area to 3–5 mm diameter discs, which yielded testable specimens across all samples. PDKs **3**–**6** exhibited the highest lap shear strength values, where oxy-functionalized PDK **5** showed a value of 25.0 MPa for (**Fig. 5b** & **Supplementary Table 5**). To quantify the benefits of oxy-functionalized PDK adhesives over their exact heteroatom-free counterparts, we calculated the lap shear strength ratios (**Fig. 5c**). Oxy-functionalized PDK **3** demonstrated hot melt adhesive properties that are 4.5 times greater than their respective heteroatom-free counterpart; PDK **5** exceed those of PDK **4**, although the difference is less pronounced compared to the ratios observed between PDK **3** and **6 (Supplementary Table 6)**. Indeed, PDK **6** was 6.3 times stronger as an adhesive than the corresponding heteroatom-free PDK **1**.

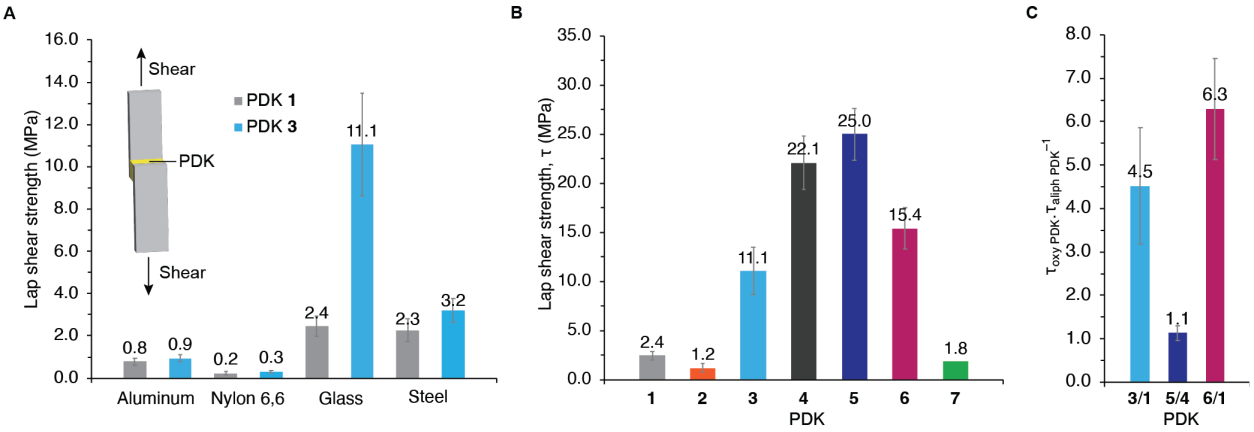

Fig. 5. Lap shear adhesion of PDK thermoplastics on different substrate. a, Lap shear adhesion on aluminum, nylon 6,6, glass, and steel surfaces of PDK **1** and **3**. **b,** Lap shear adhesion of PDK **1**–**7** on glass surfaces. **c,** Ratio of lap shear strength of oxy-functionalized PDKs to their exact heteroatom-free counterparts.

Conclusion

https://doi.org/10.26434/chemrxiv-2024-p5q4d **ORCID:** https://orcid.org/0000-0003-3925-4174 Content not peer-reviewed by ChemRxiv. **License:** CC BY-NC-ND 4.0

Our findings demonstrate that polymer reactivity can be controlled by understanding how remote functionalization to cleavable bonds influences the energetics of transition states of bond cleavage from the perspective of their reactive chain conformation. These effects are exquisitely tunable, shown here via oxy-functionalization and rate acceleration in the deconstruction of polydiketoenamines, which is immediately relevant to plastics recycling and circularity. This includes the creation of circular adhesives, where oxy-functionalization produces more strongly bonded assemblies of a diverse range of materials. From a broader perspective, the placement of heteroatoms in polymers appears to be a general strategy for promoting chain cleavage across natural and synthetic polymers, albeit with different mechanistic underpinnings, e.g., if deconstruction is spontaneous, promoted by an endogenous enzyme, or an exogenous catalyst. Yet, in all these instances, reactive polymer chain conformation manifests as a guiding principle not often considered in polymer reactivity. Moreover, the implication that a synchronicity of non-covalent interactions is necessary to attain a reactive chain conformation suggests polymer dynamics may also play an important role. From this vantage point, we see exciting opportunities to explore the macromolecular context underlying circularity principles for chemical and biological deconstruction of plastics with deep relevance to sustainability, environmental health, and the manufacturing economy.

Data availability

All data is available in the main text or the Supplementary Information.

References

1. Jehanno, C. *et al.* Critical advances and future opportunities in upcycling commodity polymers. *Nature* **603**, 803–814 (2022).
2. Coates, G. W. & Getzler, Y. D. Y. L. Chemical recycling to monomer for an ideal, circular polymer economy. *Nat. Rev. Mater.* **5**, 501–516 (2020).
3. Korley, L. T. J., Epps, T. H., Helms, B. A. & Ryan, A. J. Toward polymer upcycling-adding value and tackling circularity. *Science* **373**, 66–69 (2021).
4. Ellis, L. D. *et al.* Chemical and biological catalysis for plastics recycling and upcycling. *Nat. Catal.* **4**, 539–556 (2021).

https://doi.org/10.26434/chemrxiv-2024-p5q4d **ORCID:** https://orcid.org/0000-0003-3925-4174 Content not peer-reviewed by ChemRxiv. **License:** CC BY-NC-ND 4.0

5. Schwab, S. T., Baur, M., Nelson, T. F. & Mecking, S. Synthesis and Deconstruction of Polyethylene-type Materials. *Chem. Rev.* **124**, 2327–2351 (2024).
6. Häußler, M., Eck, M., Rothauer, D. & Mecking, S. Closed-loop recycling of polyethylene-like materials. *Nature* **590**, 423–427 (2021).
7. Eck, M. *et al.* Biodegradable High-Density Polyethylene-like Material. *Angew. Chem. Int. Ed.* **62**, e202213438 (2023).
8. Abel, B. A., Snyder, R. L. & Coates, G. W. Chemically recyclable thermoplastics from reversible-deactivation polymerization of cyclic acetals. *Science* **373**, 783–789 (2021).
9. Andhalkar, V. V. *et al.* Valorization of Lignocellulose by Producing Polyhydroxyalkanoates under Circular Bioeconomy Premises: Facts and Challenges. *ACS Sustain. Chem. Eng.* **10**, 16459–16475 (2022).
10. Fransen, K. A. *et al.* High-throughput experimentation for discovery of biodegradable polyesters. *Proc. Natl. Acad. Sci. U.S.A.* **120**, e2220021120 (2023).
11. Jang, Y.-J., Nguyen, S. & Hillmyer, M. A. Chemically Recyclable Linear and Branched Polyethylenes Synthesized from Stoichiometrically Self-Balanced Telechelic Polyethylenes. *J. Am. Chem. Soc.* **146**, 4771–4782 (2024).
12. Wu, X.-T. *et al.* Enabling Closed-Loop Circularity of "Non-Polymerizable" α, β-Conjugated Lactone towards High-performance Polyester with the Assistance of Cyclopentadiene. *Angew. Chem. Int. Ed.* **63**, e202404179 (2024).
13. Birkle, M., Mehringer, H. S., Nelson, T. F. & Mecking, S. Aliphatic Polyester Materials from Renewable 2,3-Butanediol. *ACS Sustain. Chem. Eng.* **12**, 4156–4163 (2024).
14. Nelson, T. F., Rothauer, D., Sander, M. & Mecking, S. Degradable and Recyclable Polyesters from Multiple Chain Length Bio- and Waste-Sourceable Monomers. *Angew. Chem. Int. Ed.* **62**, e202310729 (2023).
15. Zhu, J.-B., Watson, E. M., Tang, J. & Chen, E. Y.-X. A synthetic polymer system with repeatable chemical recyclability. *Science* **360**, 398–403 (2018).
16. Tang, X. & Chen, E. Y.-X. Toward Infinitely Recyclable Plastics Derived from Renewable Cyclic Esters. *Chem.* **5**, 284–312 (2019).
17. Sangroniz, A. *et al.* Packaging materials with desired mechanical and barrier properties and full chemical recyclability. *Nat. Commun.* **10**, 1–7 (2019).

https://doi.org/10.26434/chemrxiv-2024-p5q4d **ORCID:** https://orcid.org/0000-0003-3925-4174 Content not peer-reviewed by ChemRxiv. **License:** CC BY-NC-ND 4.0

18. Li, X.-L., Clarke, R. W., Jiang, J.-Y., Xu, T.-Q. & Chen, E. Y.-X. A circular polyester platform based on simple gem-disubstituted valerolactones. *Nat. Chem.* (2024) doi:10.1038/s41557-022-01077-x.
19. Shi, C. *et al.* Topology-Accelerated and Selective Cascade Depolymerization of Architecturally Complex Polyesters. *J. Am. Chem. Soc.* **146**, 9261–9271 (2024).
20. Han, X.-W. *et al.* Circular olefin copolymers made de novo from ethylene and α-olefins. *Nat. Commun.* **15**, 1462 (2024).
21. Shi, C. *et al.* High-performance pan-tactic polythioesters with intrinsic crystallinity and chemical recyclability. *Sci. Adv.* **6**, eabc0495 (2020).
22. Zhou, L., Reilly, L. T., Shi, C., Quinn, E. C. & Chen, E. Y.-X. Proton-triggered topological transformation in superbase-mediated selective polymerization enables access to ultrahigh-molar-mass cyclic polymers. *Nat. Chem.* (2024) doi:10.1038/s41557-024-01511-2.
23. Yuan, J. *et al.* 4-Hydroxyproline-Derived Sustainable Polythioesters: Controlled Ring-Opening Polymerization, Complete Recyclability, and Facile Functionalization. *J. Am. Chem. Soc.* **141**, 4928–4935 (2019).
24. Saxon, D. J., Gormong, E. A., Shah, V. M. & Reineke, T. M. Rapid Synthesis of Chemically Recyclable Polycarbonates from Renewable Feedstocks. *ACS Macro Lett.* **10**, 98–103 (2021).
25. Lamparelli, D. H. *et al.* Bicyclic Guanidine Promoted Mechanistically Divergent Depolymerization and Recycling of a Biobased Polycarbonate. *Angew. Chem. Int. Ed.* **62**, e202314659 (2023).
26. McGuire, T. M., Deacy, A. C., Buchard, A. & Williams, C. K. Solid-State Chemical Recycling of Polycarbonates to Epoxides and Carbon Dioxide Using a Heterodinuclear Mg(II)Co(II) Catalyst. *J. Am. Chem. Soc.* **144**, 18444–18449 (2022).
27. Rosetto, G., Vidal, F., McGuire, T. M., Kerr, R. W. F. & Williams, C. K. High Molar Mass Polycarbonates as Closed-Loop Recyclable Thermoplastics. *J. Am. Chem. Soc.* **146**, 8381–8393 (2024).
28. Zhao, J.-Z., Yue, T.-J., Ren, B.-H., Lu, X.-B. & Ren, W.-M. Closed-loop recycling of sulfur-rich polymers with tunable properties spanning thermoplastics, elastomers, and vitrimers. *Nat. Commun.* **15**, 3002 (2024).

https://doi.org/10.26434/chemrxiv-2024-p5q4d **ORCID:** https://orcid.org/0000-0003-3925-4174 Content not peer-reviewed by ChemRxiv. **License:** CC BY-NC-ND 4.0

29. Hsu, T.-G. *et al.* Mechanochemically accessing a challenging-to-synthesize depolymerizable polymer. *Nat. Commun.* **14**, 225 (2023).
30. Su, Y.-L. *et al.* Chemically Recyclable Polymer System Based on Nucleophilic Aromatic Ring-Opening Polymerization. *J. Am. Chem. Soc.* **145**, 13950–13956 (2023).
31. Liu, Y., Jia, Y., Wu, Q. & Moore, J. S. Architecture-Controlled Ring-Opening Polymerization for Dynamic Covalent Poly(disulfide)s. *J. Am. Chem. Soc.* **141**, 17075–17080 (2019).
32. Zhang, Q. *et al.* Dual closed-loop chemical recycling of synthetic polymers by intrinsically reconfigurable poly(disulfides). *Matter* **4**, 1352–1364 (2021).
33. Machado, T. O. *et al.* A renewably sourced, circular photopolymer resin for additive manufacturing. *Nature* **629**, 1069–1074 (2024).
34. Manker, L. P. *et al.* Performance polyamides built on a sustainable carbohydrate core. *Nat. Sustain.* **7**, 640–651 (2024).
35. Cywar, R. M. *et al.* Redesigned Hybrid Nylons with Optical Clarity and Chemical Recyclability. *J. Am. Chem. Soc.* **144**, 5366–5376 (2022).
36. Tian, J.-J. *et al.* Redesigned Nylon 6 Variants with Enhanced Recyclability, Ductility, and Transparency. *Angew. Chem. Int. Ed.* **63**, e202320214 (2024).
37. Shi, C. *et al.* Design principles for intrinsically circular polymers with tunable properties. *Chem* **7**, 2896–2912 (2021).
38. Christensen, P. R., Scheuermann, A. M., Loeffler, K. E. & Helms, B. A. Closed-loop recycling of plastics enabled by dynamic covalent diketoenamine bonds. *Nat. Chem.* **11**, 442–448 (2019).
39. He, C. *et al.* Conformational Entropy as a Means to Control the Behavior of Poly(diketoenamine) Vitrimers In and Out of Equilibrium. *Angew. Chem. Int. Ed.* **59**, 735–739 (2020).
40. Demarteau, J. *et al.* Circularity in mixed-plastic chemical recycling enabled by variable rates of polydiketoenamine hydrolysis. *Sci. Adv.* **8**, eabp8823 (2022).
41. Helms, B. A. Polydiketoenamines for a Circular Plastics Economy. *Acc. Chem. Res.* **55**, 2753–2765 (2022).
42. Demarteau, J. *et al.* Biorenewable and circular polydiketoenamine plastics. *Nat. Sustain.* **6**, 1426–1435 (2023).

https://doi.org/10.26434/chemrxiv-2024-p5q4d **ORCID:** https://orcid.org/0000-0003-3925-4174 Content not peer-reviewed by ChemRxiv. **License:** CC BY-NC-ND 4.0

43. Dailing, E. A. *et al.* Circular Polydiketoenamine Elastomers with Exceptional Creep Resistance via Multivalent Cross-Linker Design. *ACS Cent. Sci.* **10**, 54–64 (2024).
44. Epstein, A. R., Demarteau, J., Helms, B. A. & Persson, K. A. Variable Amine Spacing Determines Depolymerization Rate in Polydiketoenamines. *J. Am. Chem. Soc.* **145**, 8082–8089 (2023).
45. Pracht, P., Bohle, F. & Grimme, S. Automated exploration of the low-energy chemical space with fast quantum chemical methods. *Phys. Chem. Chem. Phys.* **22**, 7169–7192 (2020).
46. Møller, K. H., Otkjær, R. V, Hyttinen, N., Kurtén, T. & Kjaergaard, H. G. Cost-Effective Implementation of Multiconformer Transition State Theory for Peroxy Radical Hydrogen Shift Reactions. *J. Phys. Chem. A* **120**, 10072–10087 (2016).
47. Bao, J. L. & Truhlar, D. G. Variational transition state theory: theoretical framework and recent developments. *Chem. Soc. Rev.* **46**, 7548–7596 (2017).
48. Diehl, K. L. *et al.* Click and chemically triggered declick reactions through reversible amine and thiol coupling via a conjugate acceptor. *Nat. Chem.* **8**, 968–973 (2016).
49. Davis, G. J., Sofka, H. A. & Jewett, J. C. Highly Stable Meldrum's Acid Derivatives for Irreversible Aqueous Covalent Modification of Amines. *Org. Lett.* **22**, 2626–2629 (2020).
50. Zhang, V. *et al.* Tailoring dynamic hydrogels by controlling associative exchange rates. *Chem* **9**, 2298–2317 (2023).
51. Vora, N. *et al.* Leveling the cost and carbon footprint of circular polymers that are chemically recycled to monomer. *Sci. Adv.* **7**, eabf0187 (2022).
52. Demarteau, J., Vora, N., Keasling, J. D., Helms, B. A. & Scown, C. D. Lower-Cost, Lower-Carbon Production of Circular Polydiketoenamine Plastics. *ACS Sustain. Chem. Eng.* **10**, 2740–2749 (2022).
53. Rahman, A. M. *et al.* Design of tough adhesive from commodity thermoplastics through dynamic crosslinking. *Sci. Adv.* **7**, eabk2451 (2021).

https://doi.org/10.26434/chemrxiv-2024-p5q4d **ORCID:** https://orcid.org/0000-0003-3925-4174 Content not peer-reviewed by ChemRxiv. **License:** CC BY-NC-ND 4.0

Acknowledgement

This work was funded by the U.S. Department of Energy, Office of Science, Office of Basic Energy Sciences, Materials Sciences and Engineering Division under Contract No. DE-AC02- 05-CH11231 Unlocking Chemical Circularity in Recycling by Controlling Polymer Reactivity Across Scales program CUP-LBL-Helms. Data for this study was produced using computational resources provided by the Eagle HPC systems at the National Renewable Energy Laboratory (NREL), the Lawrencium HPC cluster at Lawrence Berkeley National Laboratory, and the Savio computational cluster resource provided by the Berkeley Research Computing program at the University of California, Berkeley (supported by the UC Berkeley Chancellor, Vice Chancellor for Research, and Chief Information Officer). A.R.E. was supported by the National Science Foundation Graduate Research Fellowship under Grant No. DGE 1752814. Portions of this work, including PDK synthesis, characterization, and deconstruction, were carried out as a User Project at the Molecular Foundry, which is supported by the Office of Science and Office of Basic Energy Sciences of the U.S. DOE under contract No. DE-AC02-05CH11231.

Author contributions

B.A.H. directed the study and B.A.H. and J.D. designed the experiments and wrote the manuscript. J.D. and L.J.R. synthesized and characterized the monomers and polymers, processed the polymers and conducted the kinetics experiments. J.D. performed macromolecular and thermomechanical characterization, conducted the recycling experiments and lap shear adhesion testing. N.R.C. and J.F.H. designed the lap shear adhesion testing. K.A.P. directed and K.A.P. and A.R.E. designed and executed the computational studies. All co-authors participated in data analysis and interpretation.

Competing interests

B.A.H. is an inventor on the U.S. provisional patent application 62/587,148 and B.A.H., A.E.P., J.D., and K.A.P. are inventors on U.S. provisional patent application 63/390,962, both submitted by Lawrence Berkeley National Laboratory that covers PDKs, as well as aspects of their use and recovery. B.A.H. has a financial interest in Cyklos Materials and Sepion Technologies. The other authors declare that they have no other competing interests.

https://doi.org/10.26434/chemrxiv-2024-p5q4d **ORCID:** https://orcid.org/0000-0003-3925-4174 Content not peer-reviewed by ChemRxiv. **License:** CC BY-NC-ND 4.0

Supplementary information

Methods

Supplementary Figs. 1–18

Supplementary Tables 1–6

Supplementary References 1–9

https://doi.org/10.26434/chemrxiv-2024-p5q4d **ORCID:** https://orcid.org/0000-0003-3925-4174 Content not peer-reviewed by ChemRxiv. **License:** CC BY-NC-ND 4.0

Graphical abstract

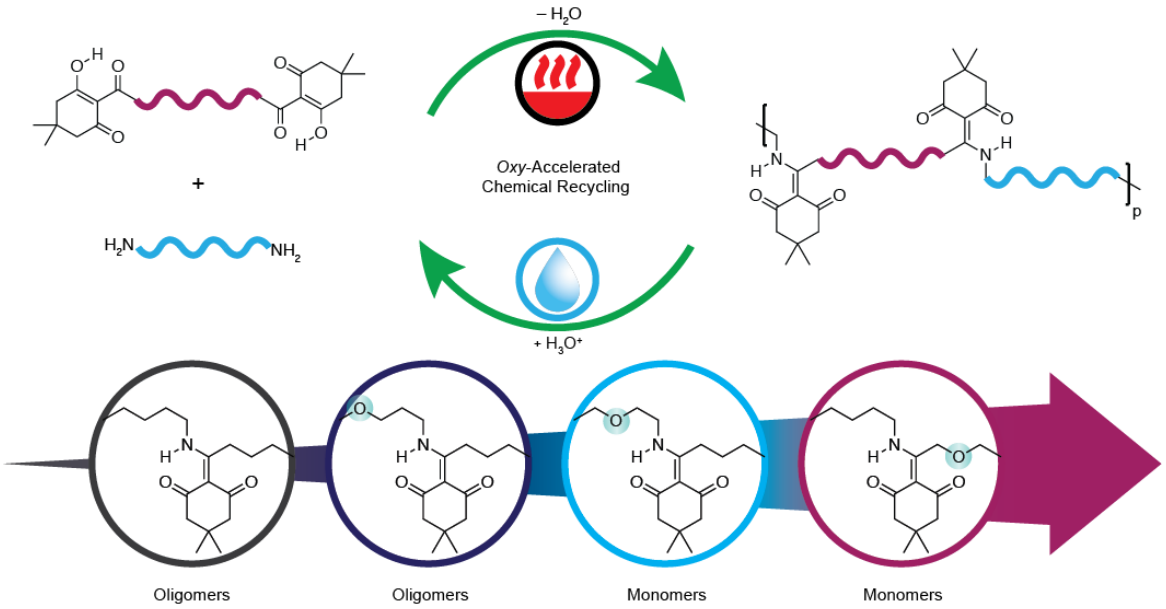

https://doi.org/10.26434/chemrxiv-2024-p5q4d **ORCID:** https://orcid.org/0000-0003-3925-4174 Content not peer-reviewed by ChemRxiv. **License:** CC BY-NC-ND 4.0